Wing Design via Numerical Optimization

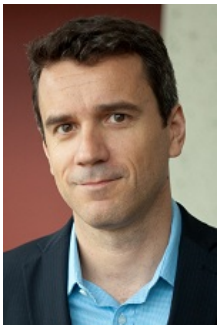

Joaquim R. R. A. Martins
Department of Aerospace Engineering
University of Michigan
Ann Arbor, MI 48109
USA
jrram@umich.edu
http://mdolab.engin.umich.edu/martins

1 Introduction

With regard to flight, the wing is arguably the most crucial component. As the legendary Boeing aircraft designer Jack Steiner put it, "The wing is where you're going to fail." In a book detailing the origins of the Boeing 747 Jumbo Jet, Irving [5] writes:

> Designing the wing involved literally thousands of decisions that could add up to an invaluable asset, a proprietary store of knowledge. A competitor could look at the wing, measure it even, and make a good guess about its internal structure. But a wing has as many invisible tricks built into its shape as a Savile Row suit; you would need to tear it apart and study every strand to figure out its secrets.

These "invisible tricks" are a reflection of the complexity involved in modeling the physics governing wing performance. The function of the wing is to provide enough lift to counteract the aircraft weight, while producing the least amount of drag (which lowers the required engine thrust). Lift and drag can be predicted through aerodynamic models that vary in sophistication and computational effort. For the flight speeds of commercial airliners (78–86% the speed of sound, or 830–925 km/h), the aerodynamic flow is compressible, and the wings usually generate shock waves. This situation, together with the fact that the wing flexibility couples the aerodynamic shape to the structural layout and sizing, contributes to the "invisible tricks" mentioned above.

We must be able to model before we optimize. To model the lift and drag accurately at transonic speeds where shocks are present requires computational fluid dynamics (CFD), which solves PDEs over the three-dimensional domain. To model the flexibility of the wing, we must couple the aerodynamic model with a structural model that predicts the deflected wing shape given the aerodynamic loads. Thus the complete wing model typically involves solving a multiphysics PDE model with at least $\mathcal{O}(10^6)$ unknowns.

The "thousands of decisions" cited in the above quote can be mapped to design variables, which involve both aerodynamic shape and structural design variables. The aerodynamic flow (and hence lift and drag) is sensitive to the slightest change in aerodynamic shape, so one must parameterize the shape with a large number of local changes.

A truly practical objective function for aircraft design is difficult to define because it depends on the balance between acquisition cost and aircraft performance. This balance depends on the business model of the particular airline, as well as on the current price of fuel. Acquisition cost is notoriously difficult to model. Aircraft performance can be modeled as operating cost, which depends on two main factors: the speed and the fuel consumption. The faster the airplane can fly, the lower the costs associated with time (e.g., crew salaries) and the more productive it can be by moving more passengers. Beyond a certain point, however, speed comes at the cost of greater fuel consumption.

When optimizing both aerodynamics and structures, we need to consider the effect of the aerodynamic shape variables and structural sizing variables on the weight, which also affects the fuel burn. Thus complex multidisciplinary trade-offs are involved in such an objective function. Numerical optimization is a powerful tool that can perform these trade-offs automatically. Aerospace engineering researchers recognized this as soon as multiphysics models for wings were available, establishing the field of multidisciplinary design optimization (MDO) [4, 12]. So far, the MDO of aircraft has involved mostly low-fidelity models that are based on either simplified physics or empirical models, with few design variables and constraints.

In this article, we show a wing design example where we tackle the compounding challenges of modeling the wing with large systems of coupled PDEs while optimizing it with respect to hundreds of design variables. We are able to meet these challenges successfully through the use of high-performance parallel computing, fast coupled PDE solvers, state-of-the-art gradient-based optimization, and an efficient approach for computing the coupled derivatives for the PDEs.

2 Optimization Problem

As we mentioned, determining the real objective function in aircraft design is difficult because of the vari-

ability in the cost of time, fuel price, and airline routes. We avoid this issue by choosing the fuel burn as the objective function to be minimized. However, the methods presented here are applicable to any other objective function.

The design variables are wing shape and structural sizing parameters, as shown in Fig. 1. Two main groups of wing shape variables exist: those that define the planform shape, and those that define the airfoil sections. The planform variables determine what the wing looks like when viewed from above. We use area, sweep, span, and taper to define the planform shape. The airfoil shape requires $\mathcal{O}(10^2)$ variables so that enough freedom is provided to reduce the aerodynamic drag. Typically, $\mathcal{O}(10^1)$ airfoil sections are distributed in the spanwise direction, each of which is allowed to change its shape independently. The wing shape is then obtained by performing an interpolation in the spanwise direction.

The shape modifications due to these shape variables are applied by using free-form deformation (FFD) [1]. This approach consists in defining a volume that encloses the wing geometry and then manipulating the surface of the volume, which changes the inside of the volume continuously. The FFD variables change both the aerodynamic surface and the structure inside the wing.

The structure inside the wing, called the wing box, usually consists of a grid of spars (laid out in the spanwise direction), ribs (laid out perpendicularly to the spars), and skins that cover the wing. All these elements are thin shells, and the structural sizing variables are the thicknesses of these shells. All sizing variables are subject to constraints on the variation in thickness of adjacent elements for manufacturing reasons.

The design variables are listed in Table 1. In addition to the wing shape and structural sizing, the angle of attack is included as a design variable in order to provide the optimizer with a way to satisfy the lift constraint.

Most of the constraints in this wing design problem are there to ensure that the wing is strong enough to sustain certain maneuvers without structural failure. We consider two maneuvers: a 2.5 g pull-up maneuver and a -1 g push-over maneuver. We prevent structural failure by constraining the stress in the structure to stay below the yield stress of the material and by constraining the structure from buckling at the allowable loads. An aggregation function is used to handle these constraints [13].

The objective functions and constraints in our wing design optimization problem (Table 1) are nonlinear,

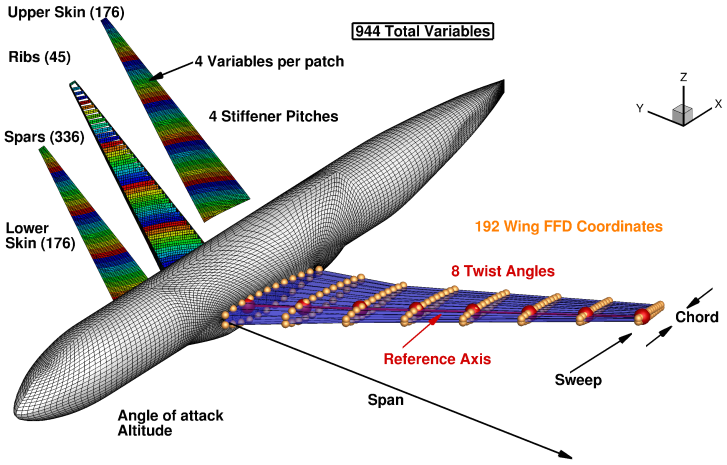

Figure 1: Wing aerostructural design variables [7].

with the exception of the adjacency and geometric constraints, which are linear. These functions are also nonconvex in general; but because of the complexity of the functions involved and the cost of the coupled PDE solutions, we currently cannot prove global optimality. However, we have studied the existence of local minima in aerodynamic shape optimization [9].

The models for the coupled aerodynamic and structural PDEs that need to be solved in order to evaluate the objective and constraints are not included explicitly in the optimization constraints because they are solved with specialized algorithms. This constitutes a reduced-space approach to a PDE-constrained optimization problem. At each optimization iteration, the aerostructural solver computes the objectives and constraints for the given set of design variables.

3 Computational Models

The physics of the wing must be modeled by coupling an aerodynamics model that computes the flow field (along with the corresponding drag and lift) and a structural model that computes the wing displacement field (along with the corresponding stress field and buckling parameters).

Here we consider high-fidelity models in the form of the Reynolds-averaged Navier–Stokes (RANS) PDEs, which can model transonic flow with shocks and provides drag estimates that include both pressure drag and skin friction drag. To solve the RANS equations, we use a finite-volume, cell-centered multiblock solver [14]. The main flow is solved by using an alternating direction implicit (ADI) method method along with geometric multigrid. A segregated Spalart–Allmaras turbulence equation is iterated with the diago-

Table 1: Aerostructural wing design optimization problem (adapted from [7]).

	Function/Variable	Quantity
minimize	Fuel burn	
with respect to	Wing span	1
	Wing sweep	1
	Wing chord	1
	Wing twist	8
	FFD control point vertical position	192
	Angle of attack at each flight condition	3
	Cruise altitude	1
	Upper and lower stiffener pitch	2
	Leading and trailing edge spar stiffener pitch	2
	Rib thickness	45
	Panel thickness for skins and spars	172
	Panel stiffener thickness for skins and spars	172
	Panel stiffener height for skins and spars	172
	Panel length for skin and spars	172
	Total number of design variables	**944**
subject to	Lift=weight at each flight condition	3
	Lift coefficient ≤ 0.525 to ensure buffet margin	1
	Leading edge thickness must not decrease	20
	Trailing edge thickness must not decrease	20
	Trailing edge spar height must not be less than 80% of the initial	20
	Wing planform area must be greater than or equal to initial	1
	Wing fuel volume must be greater than or equal to initial	1
	Panel length variable must match wing geometry	172
	Aggregate stress must not exceed the yield stress at 2.5 and -1 g	4
	Aggregate buckling must not exceed the critical value at 2.5 and -1 g	4
	Thickness must not vary by more than 2.5 mm between elements	504
	Leading and trailing edge displacement constraint	16
	Total number of constraints	**938**

nally dominant alternating direction implicit (DDADI) method.

We solve the RANS equations in the three-dimensional domain surrounding the aircraft. The computation of the drag, lift, and moment coefficients consists in the numerical integration of the flow pressure and shear stress distribution on the surface of the aircraft.

The structural solver is a parallel direct solver that uses a Schur complement decomposition [6]. For the thin-shell problems typical of aircraft structures, we often have matrix condition numbers $\mathcal{O}(10^9)$, but this solver is able to handle such problems.

The coupled aerostructural system is solved by using nonlinear block Gauss–Seidel with Aitken acceleration, which has proved to be robust for the range of flight conditions considered [8].

4 Optimization Algorithm

In selecting an optimization algorithm, two fundamental choices exist: gradient-free or gradient-based methods. Our wing design optimization application faces two compounding challenges: large numbers of design variables ($\mathcal{O}(10^2)$ or more) and a high cost of evaluating the objective and constraints (which involve the solution of coupled PDEs with $\mathcal{O}(10^6)$ variables). Since the number of iterations required by gradient-free methods does not scale well with the number of optimization variables, we use a gradient-based method. In particular, we use SNOPT [3], an implementation of the sequential quadratic programming algorithm suitable for general nonlinear constrained problems. Given the efficiency of gradient-based methods, we can address the two compounding challenges mentioned above, provided we can evaluate the required gradients efficiently.

5 Computing Gradients

With a gradient-based optimizer, the efficiency of the overall optimization hinges on an efficient evaluation of the gradients of the objective and constraint functions with respect to the design variables. Several methods are available for evaluating derivatives of PDE systems: finite differences, the complex-step method, algorithmic differentiation (forward or reverse mode), and analytic methods (direct or adjoint) [11]. The computational cost of these methods is proportional either to the number of design variables, or to the number of functions being differentiated.

Since we have a large number of design variables, the best options are the reverse-mode algorithmic differentiation or the adjoint method. In our applications we tend to use a hybrid approach that combines the adjoint method with algorithmic differentiation (both reverse and forward modes).

We now derive the adjoint method for evaluating the derivatives of a function of interest, $f(x, y(x))$ (which in our case are the objective function and constraints), with respect to the design variables x. The state variable vector y is determined implicitly by the solution of the PDEs, $R(x, y(x)) = 0$, for a given x. Using the chain rule, we calculate the gradient of f with respect to x:

$$\frac{\mathrm{d}f}{\mathrm{d}x} = \frac{\partial f}{\partial x} + \frac{\partial f}{\partial y}\frac{\mathrm{d}y}{\mathrm{d}x}. \tag{1}$$

A similar expression can be written for the Jacobian of R:

$$\frac{\mathrm{d}R}{\mathrm{d}x} = \frac{\partial R}{\partial x} + \frac{\partial R}{\partial y}\frac{\mathrm{d}y}{\mathrm{d}x} = 0.$$

We can now solve this linear system to evaluate the gradients of the state variables with respect to the design variables. Substituting this solution into the evaluation of the gradient of f (1) yields

$$\frac{\mathrm{d}f}{\mathrm{d}x} = \frac{\partial f}{\partial x} - \frac{\partial f}{\partial y}\left[\frac{\partial R}{\partial y}\right]^{-1}\frac{\partial R}{\partial x}.$$

The adjoint method consists of factorizing the Jacobian $\partial R/\partial y$ with $\partial f/\partial y$. That is, we solve the adjoint equations

$$\left[\frac{\partial R}{\partial y}\right]^{T}\psi = -\frac{\partial f}{\partial y}, \tag{2}$$

where ψ is the adjoint vector. We can then substitute the result into the total gradient equation (1),

$$\frac{\mathrm{d}f}{\mathrm{d}x} = \frac{\partial f}{\partial x} + \psi^{T}\frac{\partial R}{\partial x}, \tag{3}$$

to get the required gradient. The partial derivatives in these equations are inexpensive to evaluate, since they do not require the solution of the PDEs. The computational cost of evaluating gradients with the adjoint method is independent of the number of design variables but dependent on the number of functions of interest. Thus, this method is efficient when considering the wing design problem defined in Sec. 2, which has 944 design variables and 14 nonlinear constraints (the other 924 constraints are linear, and thus their Jacobian is constant).

The discrete adjoint solver for our CFD model was developed by forming Eqs. (2) and (3), where the partial derivatives are implemented by performing algorithmic differentiation in the relevant parts of the original code [10]. A discrete adjoint method is also implemented in our structural solver [6].

The adjoint method can be extended to coupled systems, such as the aerostructural system of equations considered here [2, 8]. For the implementation of the coupled adjoint to be efficient, we ensured that the computation of each of the partial derivatives in Eqs. (2) and (3) scales well with the number of processors [8]. The coupled adjoint equations are solved by using a coupled Krylov method, which converges faster than the linear block Gauss–Seidel method [8].

6 Wing Design Optimization

We now present the solution to the design optimization problem described in Sec. 2. The initial aircraft geometry is the Common Research Model (CRM) configuration [15], which is representative of a twin-aisle long-range airliner. The CFD solver uses a structured volume grid with 745,472 cells, resulting in more than 4.47 million degrees of freedom, while the wing box structural model has 190,710 degrees of freedom.

The planform and front views of this aircraft are shown on the left side of the geometry shown in the upper left quadrant of Fig. 2. The right side of this geometry shows the optimized aircraft. The pressure coefficient contours shown on the initial wing (left) are closely spaced in the outboard area near the trailing edge, indicating a shock wave, while the optimized wing (right) shows evenly spaced contours and no shock. The optimization reduced the drag while incurring a weight penalty, resulting in a net reduction in fuel burn. The front view of the aircraft shows the deflected shapes of the wings for both the cruise and maneuver conditions.

The upper right quadrant shows the wing structural box. The top two wings show a color map of the struc-

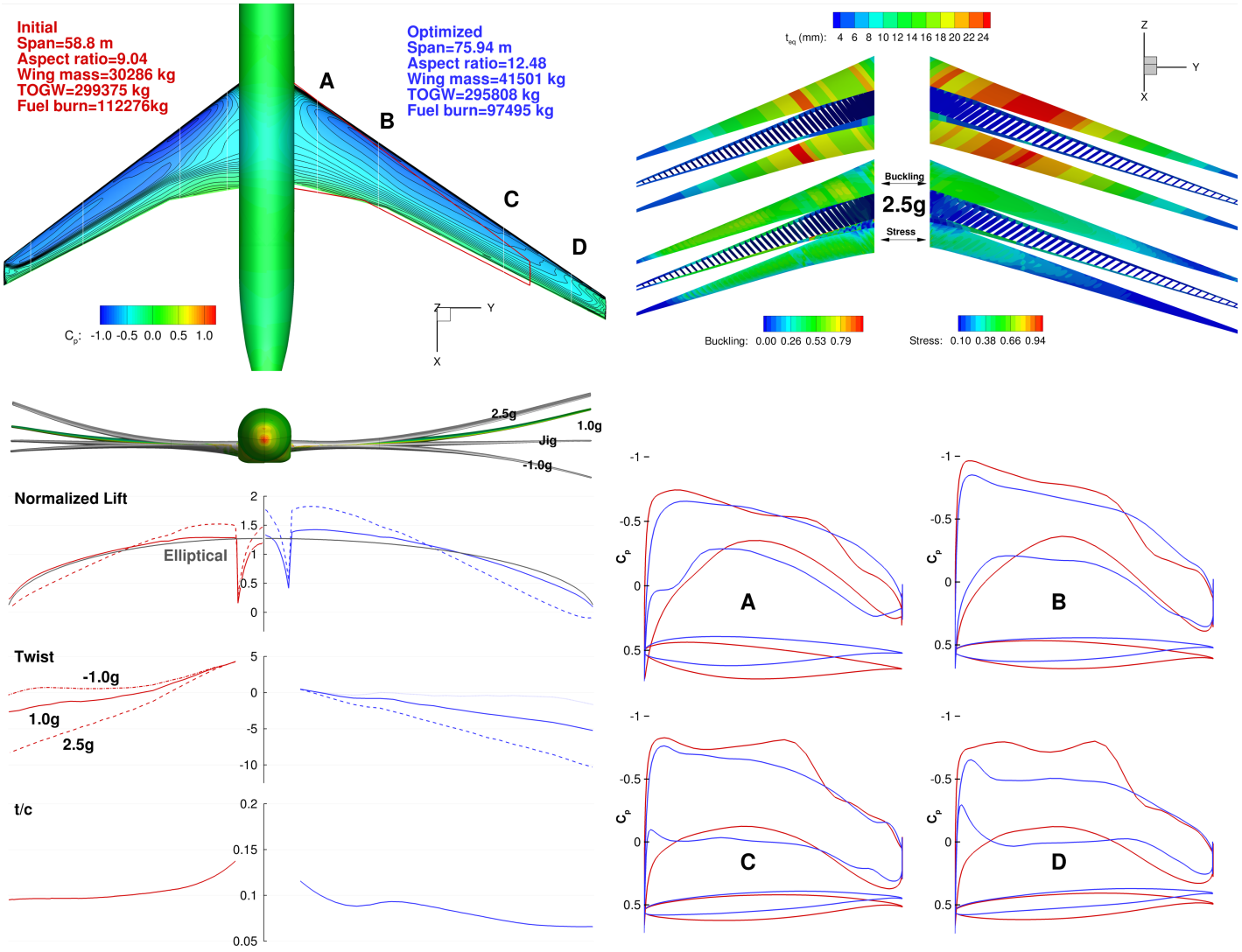

Figure 2: Initial wing design (left/red) and aerostructurally optimized wing (right/blue), showing planform view and front view (top left), wing box structure (top right), spanwise lift, twist and thickness distributions (bottom left), and airfoil sections with pressures (bottom right).

tural thickness distributions for the initial (left) and optimized (right) wing. The right wing shows the higher thicknesses that are required to strengthen the higher span wing. The bottom two wings show the values for the stress and buckling constraints, which are under the critical values (i.e., less than 1.0).

The bottom right quadrant shows four airfoil sections of the wing from the root (A) to the wingtip (D). The initial airfoils are shown in red, and the optimized airfoils are shown in blue, together with the respective pressure distributions.

7 Conclusion

In this article, we introduced a wing design problem where physics-based models of both the aerodynamics and structures were needed. Such a problem is subject to the compounding challenges of modeling the wing with large systems of coupled PDEs while optimizing the wing with respect to hundreds of design variables. We were able to tackle this problem through the use of high-performance parallel computing to solve the model PDEs, a nonlinear block Gauss–Seidel method for solving the coupled system, an SQP optimizer, and a coupled adjoint approach for computing the derivatives of the coupled PDEs. This proved to be a powerful combination that should be applicable to many other multiphysics design optimization problems.

We demonstrated these techniques in the design optimization of a large transport aircraft. The optimizer was able to tradeoff aerodynamic drag and structural

weight in just the right proportions to achieve the lowest possible fuel burn. Almost one thousand geometric shape and structural sizing variables were optimized subject to a similar number of constraints. While a number of constraints still need to be considered before these results can be directly used by aircraft manufacturers, we have demonstrated the feasibility of performing wing design optimization by using high-fidelity multiphysics models.

Acknowledgments. This work was partially supported by NASA under grant number NNX11AI19A. The author thanks Gaetan Kenway and Graeme Kennedy for the results presented in this article.

REFERENCES

[1] M. Andreoli, A. Janka, and J.-A. Désidéri. Free-form-deformation parameterization for multilevel 3D shape optimization in aerodynamics. Tech. Report 5019, INRIA, Sophia Antipolis, France, November 2003.

[2] O. Ghattas and X. Li. Domain decomposition methods for sensitivity analysis of a nonlinear aeroelasticity problem. *In. J. Comput. Fluid D.*, 11:113–130, 1998.

[3] P. E. Gill, W. Murray, and M. A. Saunders. SNOPT: An SQP algorithm for large-scale constrained optimization. *SIAM Rev.*, 47(1):99–131, 2005.

[4] R. T. Haftka. Optimization of flexible wing structures subject to strength and induced drag constraints. *AIAA J.*, 14(8):1106–1977, 1977.

[5] C. Irving. *Wide-Body—The Triumph of the 747*. William Morrow and Company, New York, 1993.

[6] G. J. Kennedy and J. R. R. A. Martins. A parallel finite-element framework for large-scale gradient-based design optimization of high-performance structures. *Finite Elem. Anal. Des.*, 87:56–73, September 2014.

[7] G. K. W. Kenway, G. J. Kennedy, and J. R. R. A. Martins. Aerostructural optimization of the common research model configuration. In *15th AIAA/ISSMO Multidiscip. Anal. Optim. Conf.*, Atlanta, GA, June 2014.

[8] G. K. W. Kenway, G. J. Kennedy, and J. R. R. A. Martins. Scalable parallel approach for high-fidelity steady-state aeroelastic analysis and derivative computations. *AIAA J.*, 52(5):935–951, May 2014.

[9] Z. Lyu, G. K. Kenway, and J. R. R. A. Martins. Aerodynamic shape optimization studies on the Common Research Model wing benchmark. *AIAA J.*, 2014. (In press).

[10] Z. Lyu, G. K. Kenway, C. Paige, and J. R. R. A. Martins. Automatic differentiation adjoint of the Reynolds-averaged Navier–Stokes equations with a turbulence model. In *21st AIAA Comput. Fluid Dyn. Conf.*, San Diego, July 2013.

[11] J. R. R. A. Martins and J. T. Hwang. Review and unification of methods for computing derivatives of multidisciplinary computational models. *AIAA J.*, 51(11):2582–2599, November 2013.

[12] J. R. R. A. Martins and A. B. Lambe. Multidisciplinary design optimization: A survey of architectures. *AIAA J.*, 51(9):2049–2075, September 2013.

[13] N. M. K. Poon and J. R. R. A. Martins. An adaptive approach to constraint aggregation using adjoint sensitivity analysis. *Struct. Multidiscip. Optim.*, 34(1):61–73, 2007.

[14] E. van der Weide, G. Kalitzin, J. Schluter, and J. J. Alonso. Unsteady turbomachinery computations using massively parallel platforms. In *Proc. 44th AIAA Aero. Sci. Meet. Exhibit*, Reno, NV, 2006. AIAA 2006-0421.

[15] J. C. Vassberg, M. A. DeHaan, S. M. Rivers, and R. A. Wahls. Development of a common research model for applied CFD validation studies, 2008. AIAA 2008-6919.

Relaxations for Some NP-Hard Problems Based on Exact Subgraphs

Franz Rendl
Institut für Mathematik
Alpen-Adria Universität Klagenfurt
Austria
Franz.Rendl@aau.at
https://campus.aau.at/org/visitenkarte.jsp?personalnr=2034

1 Max-Cut and Stable-Set

Many classical NP-complete graph optimization problems have relaxations based on semidefinite optimization. Two prominent examples are *Max-Cut* and *Stable-Set*.

We consider the Max-Cut problem in the following form. Given a symmetric matrix L of order n, find

$$z_{MC} := \max\{c^T L c : \ c \in \{-1,1\}^n\}.$$

The cut polytope CUT_n is defined as

$$\mathrm{CUT}_n := \mathrm{conv}\{cc^T : c \in \{-1,1\}^n\}.$$

Clearly, $z_{MC} = \max\{\langle L, X\rangle : X \in \mathrm{CUT}\}$. The cut polytope is contained in the spectrahedron

$$\mathrm{CORR} := \{X : \mathrm{diag}(X) = e, X \succeq 0\},$$

consisting of all correlation matrices, those semidefinite matrices having the all-ones vector e on the main diagonal. Optimizing over CORR yields one of the most well-studied semidefinite optimization problems,

$$z_{\mathrm{CORR}} := \max\{\langle L, X\rangle : X \in \mathrm{CORR}\}. \qquad (1)$$

It was introduced (in dual form) by Delorme and Poljak [7]. Goemans and Williamson [8] provided a theoretical error analysis showing that $z_{MC} \geq 0.878 \cdot z_{\mathrm{CORR}}$ for graphs with nonnegative edge weights.